Japan Journal of Research

Original Article

Density Functional Theory Study of the Second-order Nonlinear Optical Properties of Novel Fluorenone Derivatives

Yuanyuan Jia[1], Daoling Peng[2]

[1]School of Chemistry, South China Normal University, Guangzhou 510006, China

[2]Key Laboratory of Theoretical Chemistry of Environment, Ministry of Education; School of Environment, South China Normal University, Guangzhou 510006, China

Correspondence

Daoling Peng
Key Laboratory of Theoretical Chemistry of Environment, Ministry of Education; School of Environment, South China Normal University, Guangzhou 510006, China

Abstract

Based on the molecular structure of novel fluorenone derivative named FO52, a series of new molecules have been designed by extending its π-conjugated bridge and introducing electron donor or acceptor substituents. The electronic transition and second-order non-linear optical response properties of these fluorenone derivatives were theoretically studied in detail by using the density functional theory computational methods. The results showed that the non-linear optical response of the molecule FO52 can be improved by introducing five-membered heterocycles into its skeleton structure. In addition, the introduction of strong substituents results in significant enhancement of the first hyperpolarizability of molecular nonlinear optical properties. These fluorenone derivatives could be treated as excellent candidates for nonlinear optical materials due to the narrow energy gap of its frontier molecular orbitals, distinct intramolecular charge transfer character and large first hyperpolarizabilities.

- Received Date: 25 Feb 2023
- Accepted Date: 02 Mar 2023
- Publication Date: 05 Mar 2023

Introduction

Nonlinear optics (NLO) has been a hot area of modern optoelectronics since the second harmonic was observed by Franken et al. [1,2]. Nonlinear optical materials have attracted significant interest among researchers due to their broad application prospects such as optoelectronics, photonic devices, frequency doubling second harmonic generation, fiber-optic telecom communication, etc [3-7]. During the last few decades, some experimental and theoretical scientists have been invested a great deal of effort in designing and synthesizing new nonlinear optical materials at the molecular level [8-10]. Among these NLO materials, organic materials are popular over the conventional inorganic crystalline materials due to its larger NLO response, higher laser damage threshold and easier synthesis [11-14]. In the design and synthesis of organic molecules, donor/conjugated-bridge/acceptor (D-π-A) structure molecules are favored by researchers [15-17]. This special D-π-A structure promotes intramolecular charge transfer (ICT), resulting in large dipole moments and hyperpolarizabilities[18-20]. The hyperpolarizability is one of the vital parameters to evaluate the NLO properties for materials. It is necessary to explore new molecules with larger NLO response to develop novel NLO materials.

However, unimolecule with high hyperpolarizability does not always result in materials with outstanding macroscopic NLO response, because many molecules always assemble in centrosymmetric way [21,22]. Fluorenone, as an aromatic organic building block, has been usually employed as an electron acceptor in ICT molecules due to its good electron delocalization characteristics and planarity [23,24]. The fluorenone-based compounds generally seem to have a very high damage threshold. Furthermore, the centrosymmetry of fluorenone derivatives is broken owing to the introduction of the carbonyl group, and it is also gives them a permanent dipole moment that is always towards the carbonyl group. The fluorenone derivatives not only have high unimolecular hyperpolarizability, but also are easy to assemble in non-centrosymmetric ways [25,26]. These make fluorenone derivatives display great potential for application in the field of nonlinear optics.

Although multiphoton absorption in fluorenone compounds has been reported many times [27,28], little attention has been paid to their second order nonlinear optics. However, most of the study focus on the experiments of synthesis, related theoretical researches are scarce. Recently, a novel NLO molecule abbreviated as FO52 was

Citation: Jia Y, Peng D. Density Functional Theory Study of the Second-order Nonlinear Optical Properties of Novel Fluorenone Derivatives. Japan J Res. 2023;4(3):1-8.

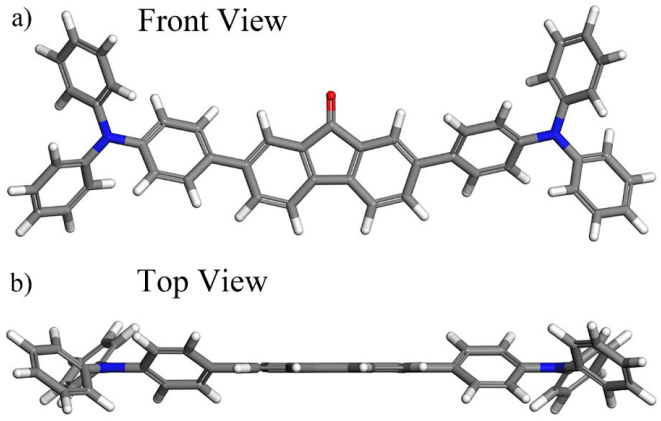

Figure 1. *Structure of the FO52 molecule, a) Front view, b) Top view.*

synthesized [29]. As illustrated in Figure 1, this molecule consists of a fluorenone core and triphenylamine donor on both sides. In order to prolong the conjugated chain length, three different five-membered heterocycles were introduced between the fluorenone core and triphenylamines of molecule FO52. Then the effects of different push-pull electron substituents on NLO properties were investigated. It is expected that this theoretical work could provide effective guidance for the synthesis of novel NLO materials.

Computational details

We first performed the basis set and functional tests. the results show that several electronic properties such as the highest occupied molecular orbital (HOMO) energies, the lowest unoccupied molecular orbital (LUMO) energies and the HOMO–LUMO energy gaps (E_{gap}) of molecule FO52 in optimized geometry at the B3LYP/6-31G(d) level are fairly closed to experimental work [29]. Therefore, it is reasonable to optimize FO52 and its derivatives at the B3LYP/6-31G(d) level. The detailed calculation results can be found in the Table S1 and S2 of supporting materials. The vibrational frequencies of all molecules are real values, which indicates that the optimized geometrical structures of these components are reliable.

It is vital to select a suitable calculation method and basis set to obtain accurate first hyperpolarizability. The conventional exchange correlation functional of DFT may overestimate the first hyperpolarizability due to its wrong asymptotic exchange potentials [30]. However, the hybrid exchange correlation functional CAM-B3LYP can solve this problem because it includes a long-range correction. To perform the functional and basis set tests, several molecules are selected as testing set. At the same basis set 6-31+G(d) level, we selected the traditional functional B3LYP [31] and four functionals with different Hartree-Fock exchange components, including CAM-B3LYP [32,33], BHandHLYP [34], M06-2X [35] and ωB97XD [36]. As shown in Figure 2, the first hyperpolarizabilities calculated by five different exchange-correlation functionals have the same variation trend. However, the functional CAM-B3LYP has been successfully applied to evaluate the NLO properties of charge transfer systems [37-40]. CAM-B3LYP was selected to evaluate the NLO properties of the present system. Besides functional tests, we also perform the basis set tests by using the CAM-B3LYP functional in combination with different basis sets including 6-31+G(d), 6-31+G(d,p), 6-31++G(d,p) and 6-311++G(d,p). As shown in Table S3, the relative errors comparing to 6-31+G(d) are about 1% which is

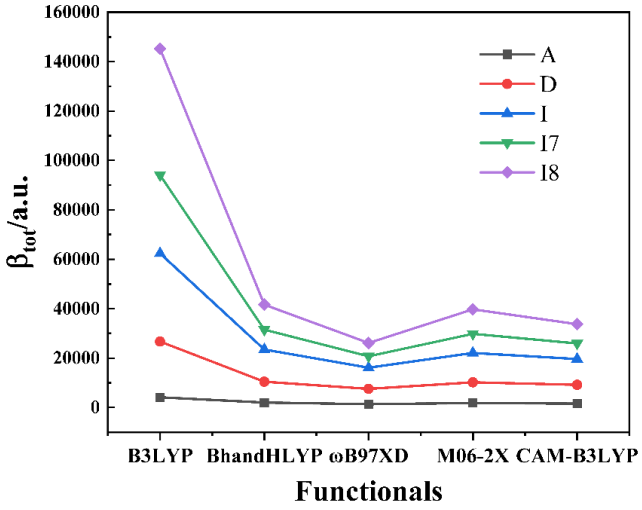

Figure 2. *The static first hyperpolarizability values of molecule A, D, I, I7, I8 obtained by employing 6-31+G(d) basis set with varies DFT funtionals.*

negligible. But other basis set are larger than 6-31+G(d) and leading to longer computational time. In order to shorten the calculation time, the basis set 6-31+G(d) was then employed in this work.

The static first hyperpolarizability are calculated according to the following equation

$$\beta_0 = \left(\beta_x^2 + \beta_y^2 + \beta_z^2\right)^{1/2} \quad (1)$$

where

$$\beta_i = \sum_{k=x,y,z} \beta_{ikk} \quad (2)$$

The Hyper-Rayleigh-Scattering (HRS) method established by Champagne and his co-workers[41] is defined as

$$\beta_{HRS}\left(-2\omega,\omega,\omega\right) = \left(\left\langle \beta_{ZZZ}^2 \right\rangle + \left\langle \beta_{ZXX}^2 \right\rangle\right)^{1/2} \quad (3)$$

Where β_{zzz}^2 and β_{zxx}^2 represent the orientational averages of β tensor components, and they also can be considered as contributed by dipolar ($\beta_{J=1}$) and octupolar ($\beta_{J=3}$) tensor components, namely

$$\beta_{HRS} = \sqrt{(\beta_{HRS})^2} = \sqrt{\left(\frac{10}{45}|\beta_{J=1}|^2 + \frac{10}{105}|\beta_{J=3}|^2\right)} \quad (4)$$

In addition, the nonlinear anisotropy parameter ρ (eq 5) is utilized to evaluate the ratio of the dipolar (eq 6) and octupolar (eq 7) contributions to the hyperpolarizability tensor.

$$\rho = \frac{|\beta_{J=3}|}{|\beta_{J=1}|} \quad (5)$$

$$\Phi_{J=1} = \frac{1}{1+\rho} \quad (6)$$

$$\Phi_{J=3} = \frac{\rho}{1+\rho} \quad (7)$$

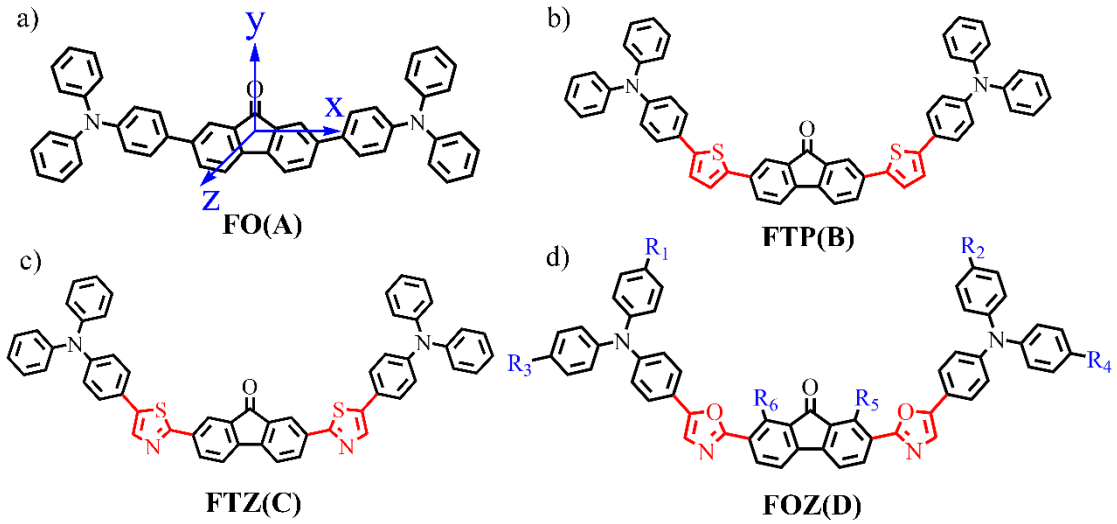

FOZ(D): R_1=R_2=R_3=R_4=R_5=R_6=H
FOZ-Me(E): R_1=R_2=R_3=R_4=CH_3, R_5=R_6=H
FOZ-OMe(F): R_1=R_2=R_3=R_4=OCH_3, R_5=R_6=H
FOZ-N(G): R_1=R_2=R_3=R_4=NH_2, R_5=R_6=H
FOZ-NMe(H): R_1=R_2=R_3=R_4=$NH(CH_3)$, R_5=R_6=H
FOZ-NMe_2(I): R_1=R_2=R_3=R_4=$N(CH_3)_2$, R_5=R_6=H
FOZ-NMe_2-Cl(I1): R_1=R_2=R_3=R_4=$N(CH_3)_2$, R_5=Cl, R_6=H
FOZ-NMe_2-2Cl(I2): R_1=R_2=R_3=R_4=$N(CH_3)_2$, R_5=R_6=Cl
FOZ-NMe_2-F(I3): R_1=R_2=R_3=R_4=$N(CH_3)_2$, R_5=F, R_6=H
FOZ-NMe_2-2F(I4): R_1=R_2=R_3=R_4=$N(CH_3)_2$, R_5=R_6=F
FOZ-NMe_2-CN(I5): R_1=R_2=R_3=R_4=$N(CH_3)_2$, R_5=CN, R_6=H
FOZ-NMe_2-2CN(I6): R_1=R_2=R_3=R_4=$N(CH_3)_2$, R_5=R_6=CN
FOZ-NMe_2-NO_2(I7): R_1=R_2=R_3=R_4=$N(CH_3)_2$, R_5=NO_2, R_6=H
FOZ-NMe_2-2NO_2(I8): R_1=R_2=R_3=R_4=$N(CH_3)_2$, R_5=R_6=NO_2

Figure 3. *Structures and notations of designed fluorenone derivatives.*

All the above calculations were carried out using the Gaussian 16 program package [42]. Furthermore, the distributions of electron and hole were done with the Multiwfn suite of programs (revision 3.7) [43]. All orbital visualization was obtained with the Multiwfn in combination with the VMD program [44].

Results and discussions

Geometric structures

As illustrated in Figure 3, the molecule FO52 synthesized in the experiment is named FO(A) in this work. In order to explore the effect of extended π-conjugated bridge on the second-order NLO properties, a five-membered heterocycle (thiophene, thiazole, oxazole) was inserted between the fluorenone core and triphenylamine on both sides, and corresponding molecules FTP(B),FTZ(C) and FOZ(D) were obtained. Then, on the basis of FOZ(D) molecule, different electron-donating groups (-CH_3, -OCH_3, -NH_2, -NH (CH_3), -$N(CH_3)_2$) were simultaneously introduced at the positions of R_1, R_2, R_3 and R_4 to obtain the corresponding molecules FOZ-Me (E), FOZ-OMe (F), FOZ-N (G). FOZ-NMe (H) and FOZ-NMe_2 (I) were used to investigate the effect of enhanced electron donor capacity on the molecular second-order NLO response. Finally, based on the molecule FOZ-NMe2(I), one or two identical electron- accepting groups (-Cl, -F, -CN, -NO_2) were introduced at the positions of R_5 and R_6 to obtain the molecules FOZ-NMe_2-Cl(I1), FOZ-NMe_2-2Cl(I2), FOZ-NMe_2-F(I3), FOZ-NMe_2-F(I3), FOZ-NMe_2-Cl(I1), FOZ-NMe_2-2Cl (I2), FOZ-NMe_2-F(I3). FOZ-NMe_2-2F(I4), FOZ-NMe_2-CN(I5), FOZ-NMe_2-2CN(I6), FOZ-NMe_2-NO_2(I7), FOZ-NMe_2-2NO_2(I8). For the sake of discussion, the corresponding abbreviations in parentheses will be mainly used for discussion below.

Frontier molecular orbital and state density

It is well known that the frontier molecular orbitals can be used to reveal the relationship between photophysical properties and geometric structures [45]. In addition, the HOMO–LUMO energy gap (E_{gap}) is one of the important parameters regulating optical properties. Compounds with smaller energy gap might contribute to more significant second-order NLO response. As depicted in Figure 4, the HOMO and LUMO energies are in the range of –4.95

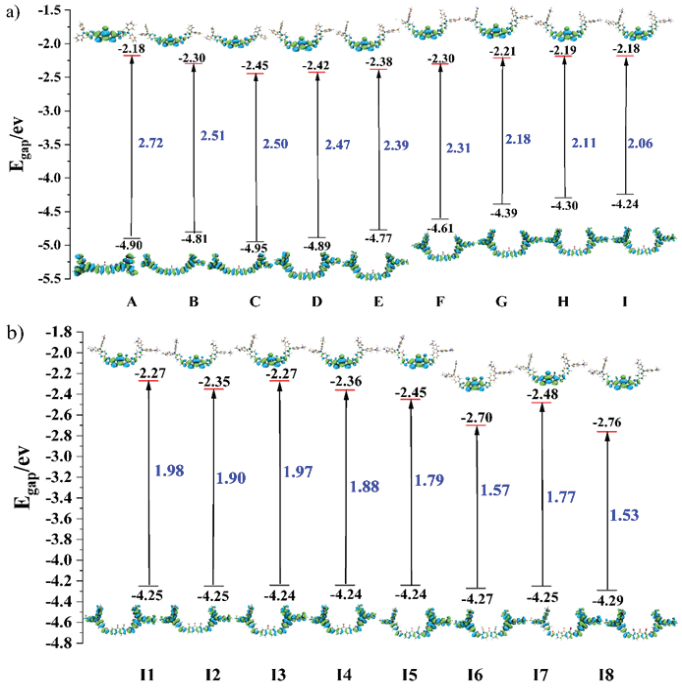

Figure 4. *Frontier molecular orbital diagrams, energy levels (eV) and HOMO–LUMO energy gaps (eV): (a) Molecules A-I, (b) Molecules I1-I8.*

to −4.24 eV and −2.76 to −2.18 eV, respectively. These energies supply the energy gap between 1.53 and 2.72 eV. The E_{gap} variation trend of molecule A-D is as follows: D(2.47eV) < C(2.50eV) < B(2.51eV) < A(2.72eV). Also the energy gap decreased due to the progressive increase in the electron-donating ability of the substituent by the following order: I(2.06eV) < H(2.11eV) < G(2.18eV) < F(2.31eV) < E(2.39eV). The E_{gap} value of unilateral substitution molecules I1, I3, I5 and I7 is 1.98, 1.97, 1.79 and 1.77eV respectively, which is smaller than molecule I(2.06eV). Similarly, the E_{gap} value of bilateral substitution molecules I2, I4, I6 and I8 is 1.90, 1.88, 1.57 and 1.53eV, respectively. Hence, incorporation of acceptor substitution is an effective way to tune the E_{gap} values. And the E_{gap} values for molecules I8 have obvious decrease, which can be attributed to the enhancement of electron-accepting ability of acceptor. In addition, it can be seen from Figure 4 that the frontier molecular orbital distributions of these molecules are similar. For molecule A-I, the HOMOs are delocalized on the entire molecular skeleton, whereas the LUMOs are mainly located on the fluorenone core, indicating that these molecules are locally excited. With regard to molecules I1-I8, their LUMO distributions are similar to those of molecule A-I, while the HOMO are more distributed on the donors' side of the fluorenone core than molecule A-I, indicating large amount of charge transfer in these molecules. In conclusion, E_{gap} can be effectively regulated by extension of conjugated bridge and enhancement of donor and acceptor intensity. In addition, these molecules have obvious intramolecular charge transfer, which might contribute to large second-order nonlinear optical response.

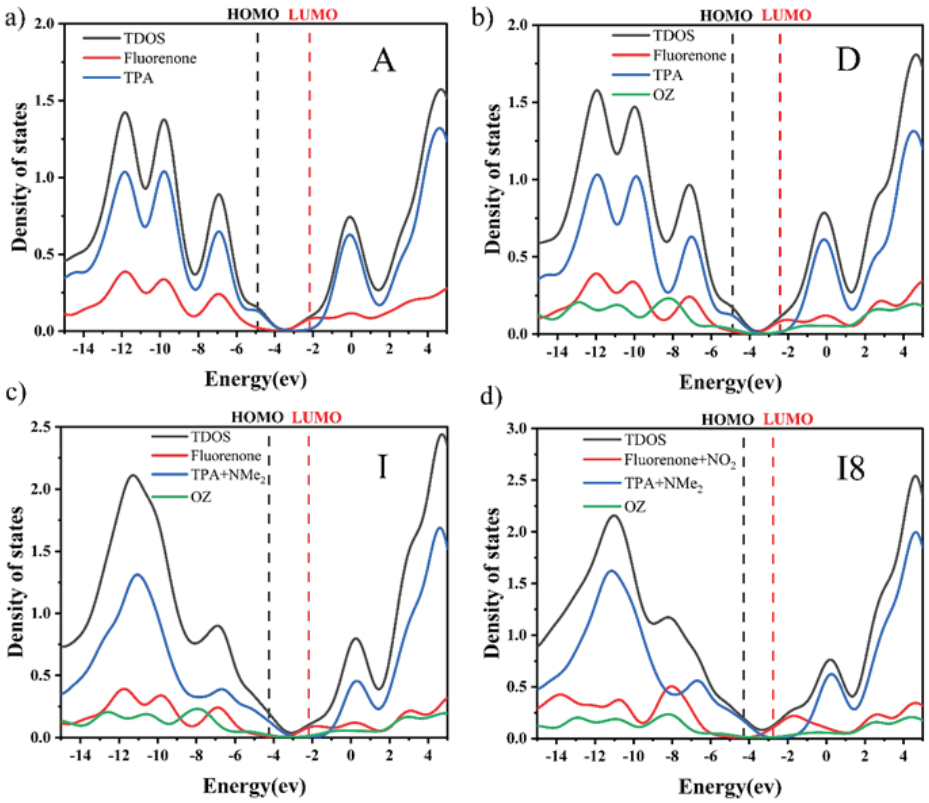

Figure 5. *Total and partial density of states of molecule A, D, I and I8.*

A more detailed study of the relationship between the geometric structures and electronic properties could be obtained by analysis of density of states. Therefore, the total density of states (TDOS) and partial density of states (PDOS) calculations of molecules A, D, I and I8 have been carried out. As described in Figure 5, molecule A is divided into fluorenone core and triphenylamines (TPA), molecule D is divided into fluorenone core, triphenylamines (TPA) and oxazole-π bridge (OZ), and molecule I is divided into fluorenone core, triphenylamines (TPA) and -NMe_2 groups, oxazole-π bridge (OZ). The molecule I8 is divided into three parts: fluorenone core and -NO2 groups, triphenylamines and- NMe_2 group, oxazole π-bridge (OZ). The results show that triphenylamines play a significant role in the formation of HOMO. However, for the LUMO, the fluorenone core is the main contribution. This phenomenon indicates that these molecules might still have obvious charge transfer after the accumulation of crystals, and the electron density is transferred to the fluorenone core, which is in good agreement with the results shown in the frontier molecular orbital diagram.

***Table 1**. Static total first hyperpolarizability (β_{tot}) and components of first hyperpolarizability (β_i) for all studied molecules.*

Molecule	β_x/a.u.	β_y/a.u.	β_z/a.u.	β_{tot}/a.u.
A	-0.5	1610.7	-0.2	1610.7
B	381.9	7307.9	552.4	7338.7
C	-205.1	7523.4	-460.2	7537.2
D	-256.7	9095.2	-224.5	9180.9
E	199.6	11492.2	872.9	11527.1
F	-51.3	14158.8	-676.5	14175.1
G	91.5	16396.2	1054.4	16430.3
H	566.9	18302.8	34.5	18311.6
I	-2.8	19598.2	930.6	19620.3
I1	323.0	20185.3	-136.4	20188.4
I2	-116.2	20146.6	2910.6	20356.1
I3	730.3	21521.9	49.5	21533.9
I4	-1246.7	23381.6	2665.9	23566.1
I5	3190.4	25263.6	5.8	25464.2
I6	-2449.4	31149.5	-5491.2	31724.5
I7	-1894.8	25844.9	1291.6	25946.4
I8	-628.4	33738.5	233.3	33745.2

Static first hyperpolarizability

The first static hyperpolarizabilities of the studied molecules A-I8 were calculated at CAM-B3LYP/6-31+G(d) level, and the results are shown in Table 1. the total first hyperpolarizability (β_{tot}) values of molecules A-D increase as the order of β_{tot}(A)< β_{tot}(B)< β_{tot}(C)< β_{tot}(D). The β_{tot} value of molecule D, which introduced oxazole as the conjugated bridge, is about 6 times that of its parent molecule A, indicating that using five-membered heterocycles to prolong the conjugated bridge is an effective method to enhance the NLO response. For molecules D-I, the order of βtot values is β_{tot}(D) <β_{tot}(E) <β_{tot}(F) <β_{tot}(G) <β_{tot}(H) <β_{tot}(I). This indicates that the stronger the electron-donating ability, the higher the β_{tot} value of the molecules, and the strong electron-donating group -NMe_2 can significantly increase the β_{tot} value. For molecules I1, I3, I5, I7 and I2, I4, I6, I8 their β_{tot} values enhance with the increased capacity of electron-withdrawing group. For the unilateral substitution, the order of β_{tot} values is β_{tot}(I1)< β_{tot}(I3)< β_{tot}(I5)< β_{tot}(I7). For the bilateral substitution, the β_{tot} values show as β_{tot}(I2)< β_{tot}(I4)< β_{tot}(I6)< β_{tot}(I8). Moreover, the β_{tot} values of molecules I2, I4, I6, I8 are larger than that of molecules I1, I3, I5, I7, showing that bilateral substitution might produces more remarkable NLO response than unilateral substitution. Besides, the β_{tot} value of molecules I8 are about three times relative to alkalide compounds Li+(calix[4]pyrrole)M− (M = Li and Na) where β_0 values of 10969 and 14772 a.u. [46]. This indicates that molecule I8 is a good potential candidate for NLO materials. In addition, the relationship between βtot and E_{gap} is analyzed. As shown in Figure 6, the variation trend of E_{gap} is opposite to that of βtot, which means that extending the conjugated bridge, introducing the electron donors and acceptors can effectively reduce the E_{gap} and obtain a larger β_{tot} value.

In order to understand the reason for the large second-order NLO response of the studied molecules, we use two-level and three-level models [47,48] for qualitative analysis. These models are derived from sum-of-state (SOS) [43,49], which is specifically expressed in the following formulas (8) and (9).

$$\beta^{sos} \propto \frac{\Delta\mu \cdot f_0}{\Delta E^3} \tag{8}$$

$$\beta^{sos} = 6\frac{\left(\mu_{0i}^{Z}\right)\Delta\mu_i^{Z}}{\Delta i^2} + 12\frac{\mu_{0i}^{Z}\mu_{0j}^{Z}\mu_{ij}^{Z}}{\Delta i\Delta j} + 6\frac{\left(\mu_{0j}^{Z}\right)\Delta\mu_j^{Z}}{\Delta j^2} \tag{9}$$

***Figure 6.** The relationship between the static first hyperpolarizability (β_{tot}) and the HOMO-LUMO energy gap (E_{gap})*

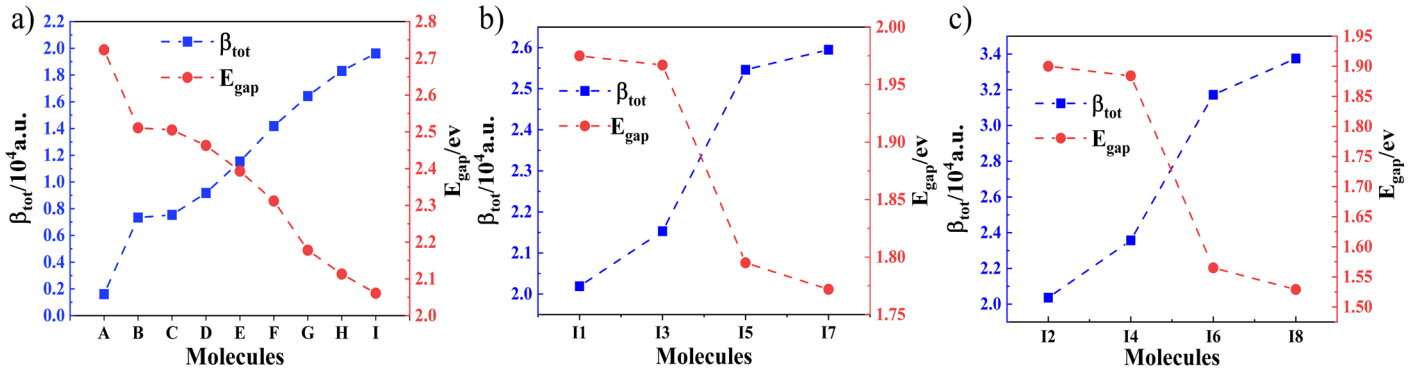

It can be clearly seen from Equation (8)) that β^{sos} value is related to the electronic excitation energy (ΔE), oscillator strength (f_0) and the difference of transition dipole moment between the ground state and the crucial excited state (Δμ). The most important factor is the excitation energy as β^{sos} is proportional to the inversion of its cubic. If two excited states are critical, they need to be discussed using the three-level formula (9). The first and third terms are the separate contributions of the two excited states, and the second term is the coupling term of the two excited states. The molecules A,B,C,D,E,F,G,H,I,I7 and I8 was used as examples to perform time-dependent density functional theory (TDDFT) calculations at the same level as the first static hyperpolarizability. First, the convergence behavior between β^{sos} and the number of excited states was tested (Figure S1). The results show that molecule A does not have one or two crucial excited states, so it does not meet the conditions of two-level or three-level model, while other molecules have converged before 50 excited states. In addition, the variation trend of β^{sos} value (a.u.) shows the same trend as β_{tot} value (Figure 6), that is B(4037) < C(4132) < D(12369) < E(14161) < F(14970) < G(15220) < H(16568) < I(17621) < I7(25189) < I8(27625). In addition, two-level or three-level model analysis revealed the crucial excited states and corresponding electronic transition energy (ΔE) of these molecules (Table 2). Molecules I7 and I8 have two main excited states. Compared with the excited states S6, S2 of molecule I7 has a lower transition energy, and excited state S2 of Molecule I8 has a lower transition energy than S5. Therefore, excited states S2 with low transition energy are mainly discussed below.

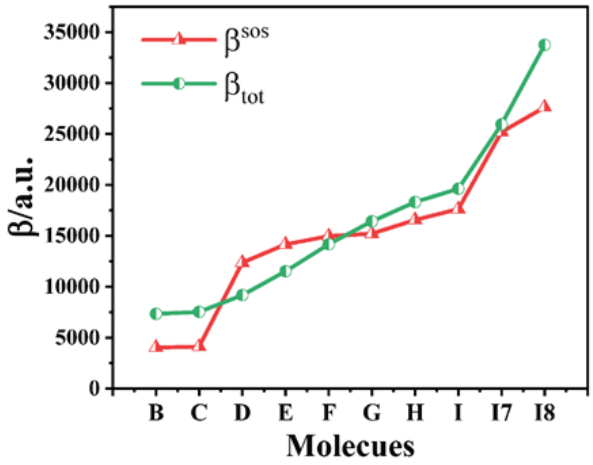

Figure 7. *Relationship between the β_{tot} value (green circle) and the corresponding βsos values (red triangle).*

Table 2. The crucial excited states and corresponding excitation energies.

Molecule	State	ΔE/eV
B	4	3.50
C	4	3.48
D	4	3.51
E	2	3.45
F	2	3.41
G	2	3.32
H	2	3.27
I	2	3.22
I7	2	2.97
	6	3.46
I8	2	2.70
	5	3.25

Table 3. The distance (D_{index} in Å) and the separation degree (t_{index} in Å) between hole and electron of corresponding excited state.

Molecule	B	C	D	E	F	G	H	I	I7	I8
D_{index}	1.274	1.368	2.341	2.623	2.894	3.367	3.656	3.965	4.338	4.540
t_{index}	-1.034	-0.832	-0.395	-0.120	0.176	0.678	0.936	1.183	1.786	2.097

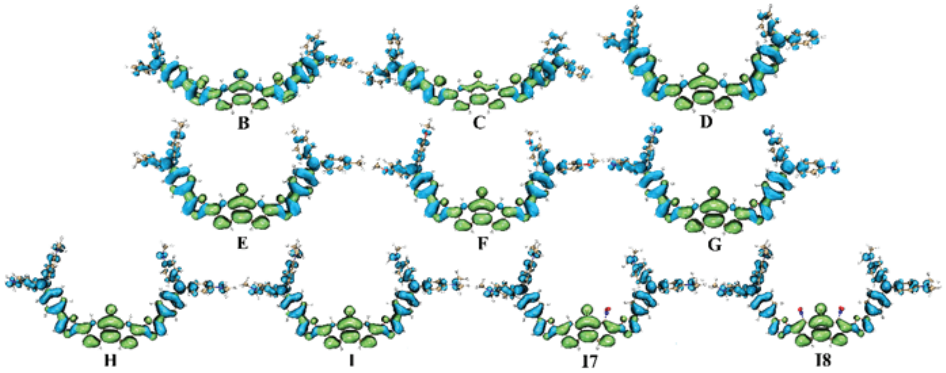

Figure 8. *Distribution of electron and hole (plotted with isovalue 0.0005)*

Distribution of electron and hole

In the case of NLO materials, the degree of charge transfer (CT) also affects the NLO response. The process of electron excitation can be graphically described as electrons and holes. Remarkably, these holes are formed where the electrons leave. To measure CT length, the distance between electron centroid and hole (D_{index}) is defined by Equation 10. The larger D_{index} is, the more obvious CT is. In addition, tindex is used to describe the degree of separation between electrons and holes in the direction of CT (Equation 11). The large tindex value usually corresponds to molecule with significant CT.

$$D_{index} = \left(D_x^2 + D_y^2 + D_z^2\right)^{1/2}$$

$$t_{index} = D_{index} - H_{CT} \quad (10)$$

$$H_{CT} = \left|H \cdot \mu_{CT}\right| \quad (11)$$

The D_{index} and t_{index} values of molecules B,C,D,E,F,G,H,I,I7 and I8 are shown in Table 3. The results show that D_{index} and t_{index} values show the same trend as β_{tot} values. In addition, combined with the distribution of electrons and holes (Figure 8), it can be shown that there is a good separation of electrons and holes in these molecules, resulting in an obvious intramolecular charge transfer (ICT), which is conducive to enhancing the second-order NLO response.

Conclusions

In this work, a series of novel D-π-A type fluorenone derivatives were investigated by DFT and TDDFT computational methods. Results including their geometric structures, frontier molecular orbitals, charge transfer directions and second-order NLO properties were obtained. The calculated results show that the HOMO-LUMO energy gap of the compounds can be effectively reduced, the intramolecular charge transfer is remarkable, and the second-order NLO response of the compounds can be enhanced by extending the conjugated bridge and enhancing the strength of the electron-donating or electron-withdrawing substituents. In addition, all designed molecules have large β_{tot} values, and the molecule FOZ-NMe_2-$2NO_2$ (I8) has the largest first hyperpolarizability (β_{tot}=33745a.u.), indicating that these molecules are potential candidates for excellent NLO materials. It is hoped that this work could provide beneficial guidance for the development of excellent NLO materials.

Acknowledgement

The authors would like to thank the National Key Research and Development Program of China (2017YFB0203403) for financial support.

References

1. Franken PA, Hill AE, Peters CW, et al. Generation of Optical Harmonics. Physical Review Letters. 1961;7(4):118-119.
2. Franken PA, Ward JF. Optical Harmonics and Nonlinear Phenomena. Reviews of Modern Physics. 1963;35(1):23-39.
3. Wang Y, Pan S. Recent development of metal borate halides: Crystal chemistry and application in second-order NLO materials. Coordination Chemistry Reviews. 2016;323: 15-35.
4. Guo J, Huang D, Zhang Y, et al. 2D GeP as a Novel Broadband Nonlinear Optical Material for Ultrafast Photonics. Laser & Photonics Reviews. 2019;13(9):1900123.
5. Wang G, Baker-Murray AA, Blau WJ. Saturable Absorption in 2D Nanomaterials and Related Photonic Devices. Laser & Photonics Reviews. 2019;13(7):1800282.
6. Zhang Y, Grady N K, Ayala-Orozco C, et al. Three-dimensional nanostructures as highly efficient generators of second harmonic light. Nano Lett. 2011;11(12): 5519-23.
7. Wu J, Li ZA, Luo J, et al. High-performance organic second- and third-order nonlinear optical materials for ultrafast information processing. Journal of Materials Chemistry C. 2020; 8(43):15009-15026.
8. Beaujean P, Bondu F, Plaquet A, et al. Oxazines: A New Class of Second-Order Nonlinear Optical Switches. J Am Chem Soc, 2016;138(15):5052-62.
9. Siva V, Bahadur SA, Shameem A, et al. Synthesis, structural, vibrational, thermal, dielectric and optical properties of third order nonlinear optical single crystal for optical power limiting applications. Journal of Molecular Structure. 2019;1191: 110-117.
10. Thakare SS, Sreenath MC, Chitrambalam S, et al. Non-linear optical study of BODIPY-benzimidazole conjugate by solvatochromic, Z-scan and theoretical methods. Optical Materials. 2017;64:453-460.
11. Chen L, Yu G, Chen W, et al. Constructing a mixed π-conjugated bridge to effectively enhance the nonlinear optical response in the Mobius cyclacene-based systems. Phys Chem Chem Phys. 2014;16(22):10933-42.
12. Wang L, Ye J T, Chen H, et al. A structure-property interplay between the width and height of cages and the static third order nonlinear optical responses for fullerenes: applying gamma density analysis. Phys Chem Chem Phys. 2017;19(3):2322-2331.
13. Rajeshirke M, Sreenath MC, Chitrambalam S, et al. Enhancement of NLO Properties in OBO Fluorophores Derived from Carbazole–Coumarin Chalcones Containing Carboxylic

Acid at the N-Alykl Terminal End. The Journal of Physical Chemistry C. 2018;122(26): 14313-14325.

14. Gao F W, Xu H L, Muhammad S, et al. Stimulating intra- and intermolecular charge transfer and nonlinear optical response for biphenalenyl biradicaloid dimer under an external electric field. Phys Chem Chem Phys. 2018;20(27): 18699-18706.
15. Reeve J E, Anderson H L, Clays K. Dyes for biological second harmonic generation imaging. Phys Chem Chem Phys. 2010;12(41):13484-98.
16. Sun Z-B, Li S-Y, Liu Z-Q, et al. Triarylborane π -electron systems with intramolecular charge-transfer transitions. Chinese Chemical Letters. 2016;27(8):1131-1138.
17. Shen H, Li Y, Li Y. Self-assembly and tunable optical properties of intramolecular charge transfer molecules. Aggregate. 2020;1(1): 57-68.
18. Li Y, Liu T, Liu H, et al. Self-assembly of intramolecular charge-transfer compounds into functional molecular systems. Acc Chem Res. 2014;47(4):1186-98.
19. Roy RS, Nandi PK. Exploring bridging effect on first hyperpolarizability. RSC Advances. 2015;5(125): 103729-103738.
20. Ma NN, Sun SL, Liu CG, et al. Quantum chemical study of redox-switchable second-order nonlinear optical responses of D-π-A system BNbpy and metal Pt(II) chelate complex. J Phys Chem A. 2011;115(46): 13564-72.
21. Xu J, Wen L, Zhou W, et al. Asymmetric and symmetric dipole–dipole interactions drive distinct aggregation and emission behavior of intramolecular charge-transfer molecules. The Journal of Physical Chemistry C. 2009;113(15): 5924-5932.
22. Xu J, Liu X, Lv J, et al. Morphology transition and aggregation-induced emission of an intramolecular charge-transfer compound. Langmuir. 2008;24(8): 4231-4237.
23. Cheng J-Z, Lin C-C, Chou P-T, et al. Fluorene as the π–spacer for new two-photon absorption chromophores. Tetrahedron. 2011;67(4):734-739.
24. Mongin O, Porres L, Charlot M, et al. Synthesis, fluorescence, and two-photon absorption of a series of elongated rodlike and banana-shaped quadrupolar fluorophores: a comprehensive study of structure-property relationships. Chemistry. 2007;13(5): 1481-98.
25. Duan Y, Ju C, Yang G, et al. Aggregation Induced Enhancement of Linear and Nonlinear Optical Emission from a Hexaphenylene Derivative. Advanced Functional Materials. 2016;26(48): 8968-8977.
26. Semin S, Li X, Duan Y, et al. Nonlinear Optical Properties and Applications of Fluorenone Molecular Materials. Adv Optical Mater. 2021;9:2100327
27. Huang T-H, Li X-C, Wang Y-H, et al. Effects of π-spacers on the linear and nonlinear optical properties of novel fluorenone-based D–π–A–π–D type conjugated oligomers with different donors. Optical Materials. 2013;35(7): 1373-1377.
28. Huang T-H, Yang D, Kang Z-H, et al. Linear and nonlinear optical properties of two novel D–π–A–π–D type conjugated oligomers with different donors. Optical Materials. 2013;35(3): 467-471.
29. Wu X, Xiao J, Han Y, et al. An investigation of broadband optical nonlinear absorption and transient nonlinear refraction in a fluorenone-based compound. RSC Advances. 2021; 11(26): 15952-15958.
30. Van Gisbergen S, Schipper P, Gritsenko O, et al. Electric field dependence of the exchange-correlation potential in molecular chains. Physical review letters. 1999;83(4): 694.
31. Becke AD. Density-functional thermochemistry. I. The effect of the exchange-only gradient correction. The Journal of Chemical Physics. 1992;96(3):2155-2160.
32. Iikura H, Tsuneda T, Yanai T, et al. A long-range correction scheme for generalized-gradient-approximation exchange functionals. The Journal of Chemical Physics. 2001;115(8): 3540-3544.
33. Yanai T, Tew D P, Handy N C. A new hybrid exchange–correlation functional using the Coulomb-attenuating method (CAM-B3LYP). Chemical Physics Letters. 2004;393(1-3): 51-57.
34. Zhao Y, Truhlar D G. The M06 suite of density functionals for main group thermochemistry, thermochemical kinetics, noncovalent interactions, excited states, and transition elements: two new functionals and systematic testing of four M06-class functionals and 12 other functionals. Theoretical Chemistry Accounts. 2007;120(1-3): 215-241.
35. Becke AD. A new mixing of Hartree–Fock and local density-functional theories. The Journal of Chemical Physics. 1993;98(2): 1372-1377.
36. Lazrak M, Toufik H, Bouzzine S M, et al. Bridge effect on the charge transfer and optoelectronic properties of triphenylamine-based organic dye sensitized solar cells: theoretical approach. Research on Chemical Intermediates. 2020;46(8): 3961-3978.
37. He H-M, Li Y, Yang H, et al. Efficient External Electric Field Manipulated Nonlinear Optical Switches of All-Metal Electride Molecules with Infrared Transparency: Nonbonding Electron Transfer Forms an Excess Electron Lone Pair. The Journal of Physical Chemistry C. 2016;121(1): 958-968.
38. Sun WM, Wu D, Li Y, et al. A theoretical study on novel alkaline earth-based excess electron compounds: unique alkalides with considerable nonlinear optical responses. Phys Chem Chem Phys. 2015;17(6): 4524-32.
39. Sun WM, Wu D, Li Y, et al. Substituent effects on the structural features and nonlinear optical properties of the organic alkalide Li+ (calix[4]pyrrole)Li. Chemphyschem. 2013;14(2): 408-16.
40. Wang SJ, Li Y, Wang YF, et al. Structures and nonlinear optical properties of the endohedral metallofullerene-superhalogen compounds Li@C60-BX4 (X = F, Cl, Br). Phys Chem Chem Phys. 2013;15(31): 12903-10.
41. Castet F, Bogdan E, Plaquet A, et al. Reference molecules for nonlinear optics: a joint experimental and theoretical investigation. J Chem Phys. 2012;136(2): 024506.
42. Frisch M, Trucks G, Schlegel H, et al. Gaussian 16, revision B. 01; Wallingford, CT, 2016.
43. Lu T, Chen F. Multiwfn: a multifunctional wavefunction analyzer. J Comput Chem. 2012;33(5): 580-92.
44. Humphrey W, Dalke A, Schulten K. VMD: visual molecular dynamics. Journal of molecular graphics. 1996;14(1):33-38.
45. Hadji D, Brahim H. Structural, optical and nonlinear optical properties and TD-DFT analysis of heteroleptic bis-cyclometalated iridium(III) complex containing 2-phenylpyridine and picolinate ligands. Theoretical Chemistry Accounts. 2018;137(12).
46. Chen W, Li Z-R, Wu D, et al. Nonlinear optical properties of alkalides Li+ (calix [4] pyrrole) M-(M= Li, Na, and K): alkali anion atomic number dependence. Journal of the American Chemical Society. 2006;128(4): 1072-1073.
47. Oudar JL, Chemla DS. Hyperpolarizabilities of the nitroanilines and their relations to the excited state dipole moment. The Journal of Chemical Physics. 1977;66(6): 2664-2668.
48. Oudar J L. Optical nonlinearities of conjugated molecules. Stilbene derivatives and highly polar aromatic compounds. The Journal of Chemical Physics. 1977;67(2): 446-457.
49. Sasagane K, Aiga F, Itoh R. Higher-order response theory based on the quasienergy derivatives: The derivation of the frequency-dependent polarizabilities and hyperpolarizabilities. The Journal of Chemical Physics. 1993;99(5): 3738-3778.

Supplemental Information

Table S1. *Calculated HOMO (eV), LUMO (eV) energies and E_{gap}(eV) of molecule FO52 with the same functional B3LYP combined with different basis sets.*

	Basis Sets	HOMO/eV	Error/%	LUMO/eV	Error/%	E_{gap}
Exp.	-	-4.91	-	-2.19	-	2.72
Cal.	6-31G	-4.92	-0.2	-2.31	-5.5	2.61
	6-31+G	-5.19	-5.7	-2.65	-21.0	2.54
	6-31G(d)	-4.90	0.2	-2.18	0.5	2.72
	6-31+G(d)	-5.19	-5.7	-2.55	-16.4	2.64
	6-31+G(d,p)	-5.20	-5.9	-2.56	-16.9	2.64
	6-31++G(d,p)	-5.20	-5.9	-2.55	-16.4	2.65
	6-311++G(d,p)	-5.25	-6.9	-2.58	-17.8	2.67

Table S2. *Calculated HOMO (eV), LUMO (eV) energies and E_{gap}(ev) of molecule FO52 with the same basis set 6-31G(d) combined with different functionals.same functional B3LYP combined with different basis sets.*

	Functionals	HOMO/eV	Error/%	LUMO/eV	Error/%	Egap
Exp.	-	-4.91	-	-2.19	-	2.72
Cal.	B3LYP	-4.90	0.2	-2.18	0.5	2.72
	BhandHLYP	-5.95	-21.2	-1.35	38.4	4.60
	ωB97XD	-6.72	-36.9	-0.44	79.9	6.28
	M06-2X	-6.09	-24.3	-1.32	39.7	4.77
	CAM-B3LYP	-6.15	-25.3	-0.96	56.2	5.19

Table S3. *The static first hyperpolarizability values of molecules A,D,I,I7,I8 obtained by employing CAM-B3LYP functional with varies basis sets.*

Molecule	Basis sets	β_{tot}/a.u.	error(%)
A	6-31+G(d)	1610.7	-
	6-31+G(d,p)	1607.2	0.2
	6-31++G(d,p)	1599.1	0.7
	6-311++G(d,p)	1593.2	1.0
D	6-31+G(d)	9180.9	-
	6-31+G(d,p)	9131.7	0.5
	6-31++G(d,p)	9094.3	0.9
	6-311++G(d,p)	9270.3	1.0
I	6-31+G(d)	19620.3	-
	6-31+G(d,p)	19653.7	0.2
	6-31++G(d,p)	19401.9	1.0
	6-311++G(d,p)	19512.2	0.6
I7	6-31+G(d)	25946.4	-
	6-31+G(d,p)	25985.7	0.2
	6-31++G(d,p)	25733.2	0.8
	6-311++G(d,p)	26018.3	0.3
I8	6-31+G(d)	33745.2	-
	6-31+G(d,p)	33795.1	0.2
	6-31++G(d,p)	33541.9	0.6
	6-311++G(d,p)	34054.3	0.9

Supplemental Information

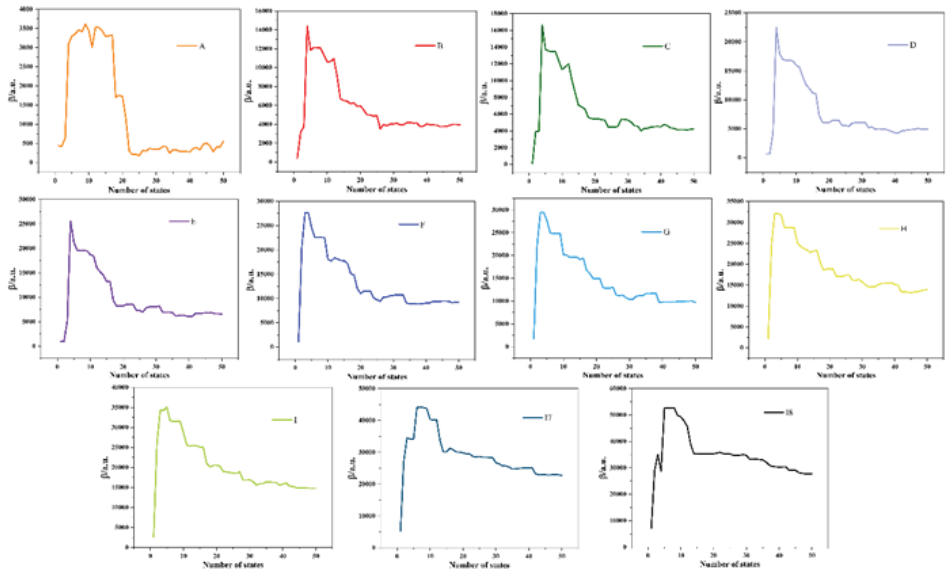

Figure S1. *Convergent behavior of molecules A-I and molecules I7, I8 on the first 50 excited states of the TDDFT calculation*